Earthquakes and Structures, *Vol. 8, No. 3 (2015) 639-663*
DOI: http://dx.doi.org/10.12989/eas.2015.8.3.639

Reduced record method for efficient time history dynamic analysis and optimal design

A. Kaveh[*1], A.A. Aghakouchak[2a] and P. Zakian[2b]

[1]*Department of Civil Engineering, Iran University of Science and Technology, Narmak, Iran*
[2]*Department of Civil and Environmental Engineering, Tarbiat Modares University, Tehran, Iran*

(Received March 15, 2014, Revised July 13, 2014, Accepted August 20, 2014)

Abstract. Time history dynamic structural analysis is a time consuming procedure when used for large-scale structures or iterative analysis in structural optimization. This article proposes a new methodology for approximate prediction of extremum point of the response history via wavelets. The method changes original record into a reduced record, decreasing the computational time of the analysis. This reduced record can be utilized in iterative structural dynamic analysis of optimization and hence significantly reduces the overall computational effort. Design examples are included to demonstrate the capability and efficiency of the Reduced Record Method (RRM) when utilized in optimal design of frame structures using meta-heuristic algorithms.

Keywords: seismic loading; time history dynamic analysis; structural optimization; wavelets; computational time reduction; improved harmony search (IHS)

1. Introduction

Time history dynamic analysis of structures is a time consuming process, particularly when large-scale structures or iterative analysis such as structural design optimization are under consideration. Furthermore, this analysis often leads to an overestimate design, thus an optimization procedure can be useful in design of structures subjected to time history loading.

Wavelet transforms are recognized as a fundamental tool for various signal-processing applications such as image processing, sound processing, earthquake accelerogram processing, ocean wave processing, etc. Wavelet transforms have been applied in many fields, some of these applications are presented in Gurley and Kareem (1999). Wavelet analysis is a technique of great interest for the analysis and approximation of non-stationary signals. One of the applications of the wavelets, which this paper focuses on it, is their utilization for generating an approximate earthquake record from an original earthquake record in order to carry out approximate and efficient time history analysis of structures with cost effective computational time (Salajegheh *et al*. 2005, Salajegheh and Heidari 2004, 2005).

*Corresponding author, Professor, E-mail: alikaveh@iust.ac.ir
[a]Professor
[b]Ph.D. Student

http://www.techno-press.org/?journal=eas&subpage=7 ISSN: 2092-7614 (Print), 2092-7622 (Online)

Optimal structural design is usually implemented to determine the design variables so as to attain an optimum structural weight or cost, while the design criteria are satisfied (Kaveh and Zakian 2012). Recently, some investigators developed meta-heuristic algorithms for structural optimization; Gholizadeh and Barzegar (2013) used a sequential harmony search algorithm for shape optimization of structures with frequency constraints; Kaveh and Zolghadr (2014) optimized truss structures with natural frequency constraints using Democratic PSO. There are a number of other papers which discuss structural design optimization using dynamic analysis. Kocer and Arora (1999) used simulated annealing and genetic algorithms for design optimization of frames with nonlinear time history analysis, Cheng *et al*. (2000) employed the game theory and genetic algorithm for multi-objective optimization of 2D frames under seismic loading, Zou and Chan (2005) proposed the use of an optimality criteria based dynamic optimal design of 2D concrete frames. Prendes Gero *et al*. (2005, 2006) employed a modified elitist genetic algorithm for dynamic design optimization of 3D steel structures. Salajegheh and Heidari (2004, 2005a, 2005b) utilized wavelets, neural network for efficient dynamic analysis and genetic algorithm for optimal design of skeletal structures under seismic loading. Gholizadeh and Salajegheh (2009) employed a meta-modeling based real valued PSO algorithm for optimizing structures under time history loading. Gholizadeh and Samavati (2011) proposed a hybrid methodology for optimal dynamic design of structures. Kaveh *et al*. (2012) performed time-history analysis based optimal design of space trusses using an evolution strategy approach, neural network and wavelets. Kaveh and Zakian (2014) improved BA optimizer and then employed it for various optimization problems incorporating static, dynamic and eigenvalue analysis subjected to different constraints. Kaveh and Zakian (2013) performed optimal design of steel moment and shear frames under seismic loading using two meta-heuristic algorithms considering stress constraints via simultaneous static-dynamic structural analysis.

In this article, a new methodology is proposed for prediction of extremum point of response history via wavelets. This method changes original record into a reduced record which can reduce computational effort. The proposed reduced record can be utilized for iterative structural dynamic analysis of optimization and hence substantially reduce overall computational effort.

This article is organized as follows: section 2 is a brief introduction to wavelets, and describes approximate time history analysis of structures using wavelets. The proposed so-called *reduced record method* is discussed in section 3, the improved harmony search meta-heuristic algorithm (optimizer) is explained in section 4. Section 5 presents the formulation of the dynamic design optimization of the skeletal structures. Section 6 and section 7 provide the design examples and conclusions, respectively.

2. Wavelets

2.1 Preliminary

Wavelets are considered as a modern signal processing tool. Similar to Fourier analysis which decomposes a signal into sine waves of various frequencies, wavelet analysis decomposes a signal into shifted and scaled versions of the original (or *mother*) wavelet. There are some important differences between Fourier analysis and wavelets. Fourier basis functions are localized in frequency but not in time. This means that although we might be able to specify all the frequencies present in a signal, but we do not know when they happen. Wavelets have localization ability in both frequency/scale (with dilations) and in time (with translations). This localization is an advantage in many cases. Second, many classes of functions can be represented by wavelets in a more compact way. For instance, functions with discontinuities and functions with sharp spikes usually take significantly fewer wavelet basis functions than sine-cosine basis functions to attain a comparable approximation. Therefore, wavelets are superior for representing functions that have discontinuities and sharp peaks. They are also more efficient for accurate decomposition and reconstruction of finite, non-periodic and non-stationary signals. They are also suitable for approximating piecewise smooth signals.

Another drawback of the Fourier Transform (FT) is that it cannot separate the low and high frequencies. In WT the use of a fully scalable window solves the signal-cutting problem. The window is shifted along the signal and for every position the spectrum is calculated. Then this process is repeated many times with a slightly shorter (or longer) window for every new cycle. At the end the result will be a set of time-frequency representations of the signal, all with different resolutions. Due to this set of representations it is called a multi-resolution analysis. Wavelets are defined in continuous and discrete forms. Here, the discrete form is defined and utilized.

2.2 Discrete wavelet transform

A wavelet transform is defined by a two-parameter family of functions. It can be expressed as

$$s(x) = \sum_{\alpha,\beta} DWT_{\alpha,\beta}\psi_{\alpha,\beta}(x), \qquad DWT_{\alpha,\beta} = \int_{-\infty}^{+\infty} s(x)\psi_{\alpha,\beta}(x)\,dx, \tag{1}$$

where α and β are integers, the functions $\psi_{\alpha,\beta}(x)$ are the wavelet expansion functions and two-parameter expansion coefficients $DWT_{\alpha,\beta}$ are called the Discrete Wavelet Transform (DWT) coefficients of $s(x)$.

The wavelet basis functions can be computed from a function $\psi(x)$ called the generating or mother wavelet through dilation, α and translation β, parameters

$$\psi_{\alpha,\beta}(x) = 2^{-\frac{\alpha}{2}}\psi(2^{-\alpha}x - \beta) \tag{2}$$

Mother wavelet function is not unique, but it must satisfy some conditions. If a scaling function $\varphi(x)$ is considered

$$\varphi(x) = \sqrt{2}\sum_k L_k\,\varphi(2x-k), \tag{3}$$

where L_k is filter coefficients of half band low-pass filters, the mother wavelet is related to the scaling function as follows

$$\psi(x) = \sqrt{2}\sum_k H_k\,\varphi(2x-k), \qquad H_k = (-1)^k L_{1-k}\,. \tag{4}$$

H_k is filter coefficients of half band high-pass filters. m-level wavelet decomposition is determined by

$$s_m(x) = \sum_k [a_{m+1,k}\varphi_{m+1,k}(x) + \sum_{\beta}^{m} d_{\beta+1,k}\psi_{\beta+1,k}(x)], \tag{5}$$

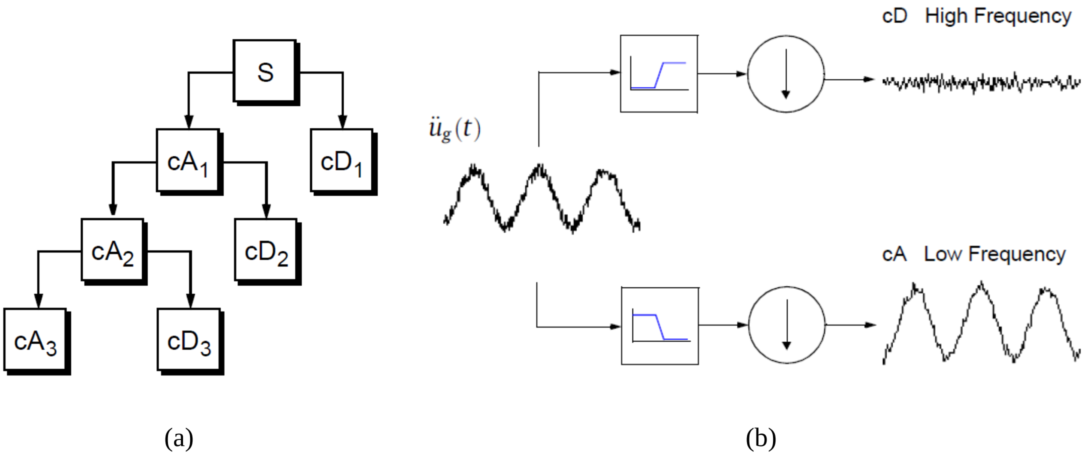

Fig. 1 Wavelet decomposition: (a) multi-level decomposition (b) a single level decomposition details of an earthquake record

In which coefficients $a_{\beta+1,n}$ and $d_{\beta+1,n}$ at scale β+1 are given by

$$a_{\beta+1,n} = \sum_k a_{\beta,k} L_{k-2n}, \qquad d_{\beta+1,n} = \sum d_{\beta,k} H_{k-2n}. \tag{6}$$

2.3 Time history analysis using wavelets

Dynamic analysis of the structures under the original earthquake record is usually a time consuming process. Recently, a method was suggested for rapid approximate time history dynamic analysis of skeletal structures (Salajegheh and Heidari 2005a). In this method, an accelerogram is decomposed using Fast Wavelet Transform (FWT) and transformed into a record with a smaller points and the dynamic analysis of structures is performed subjected to this reduced points. It should be noted that these points are corresponding to time steps or time points of an earthquake record. Fig. 1 shows the scheme for decomposition process of an earthquake accelerogram. The first part of coefficients (cA) contains the low frequency of the signal, and the other (cD) contains the high frequency of the signal. The low frequency content is the most important part because most of the earthquake energy input is of its and most of the commonly used structures are along with low natural frequencies, on the other hand, general properties of a signal are detected by this part. So, this part is used for dynamic analysis of structures. A multilevel decomposition of the signal is achieved by an iterative decomposition process. The low-pass filtered output signal is used as input record. The decomposition process can be inversed and the original record can be computed. This process is called *Inverse Discrete Wavelet Transform* (IDWT).

Fundamental steps of this method:

I) Decompose the earthquake record until a target level.

II) Use low-frequency part coefficients for dynamic analysis and modify the time intervals of time history analysis based on the selected decomposed record.

III) After dynamic analysis, use IDWT to determine the response of the structure in the original space (a time point number equal to time point number of original record).

3. Proposed reduced record method

3.1 New approach for approximate dynamic analysis using wavelets

There are two problems with using coefficient record for dynamic analysis. Firstly, after decomposition of the record to coefficient record, due to the *downsampling* process, time interval of the new record should be changed into a larger value. For instance, number of time points of El Centro record and cA1, cA2 and cA3 become 2688, 1344, 672 and 336, respectively. Thus, time intervals are taken as 0.02, 0.04, 0.08 and 0.16, respectively, because during each decomposition level half of the points are assigned to low frequency part and another half of the points are assigned to high frequency part. Also, it depends on the selected *mother wavelet*, i.e., sometimes decomposed signal is shifted or the number of points are more/less than aforementioned time points numbers which is expected. As a result, time intervals of the time history analysis cannot be attained easily based on above descriptions.

Secondly, the frequency content of coefficient records cannot be assessed and compared, because lengths (number of time points) of these records are different with original record and they are scaled as well.

In the present study, from *Daubechies wavelet family*, *Db2* has been selected to decompose the earthquake record. Here, the approximate record is proposed for dynamic analysis. Approximate record is a record which is created from its coefficient record by *upsampling* process (Fig. 2) this record has a length of equal to original record, for every considered decomposition level. As an example, A3 is an approximate record corresponding to cA3 coefficient record. Fig. 3 illustrates the El Centro record and its approximate records A1, A2 and A3. All of them have identical point numbers and after each decomposition level, every record becomes smoother than before. Although they have identical time point number, but for the reason of smoothness one can read them with different time steps, e.g., A1, A2 and A3 records can be used with 0.04, 0.08 and 0.16 time steps for any *mother wavelet* in order to fulfill time history analysis. Fig. 4 shows the frequency content of those records. Thus, frequency content of them may be compared. Finally,

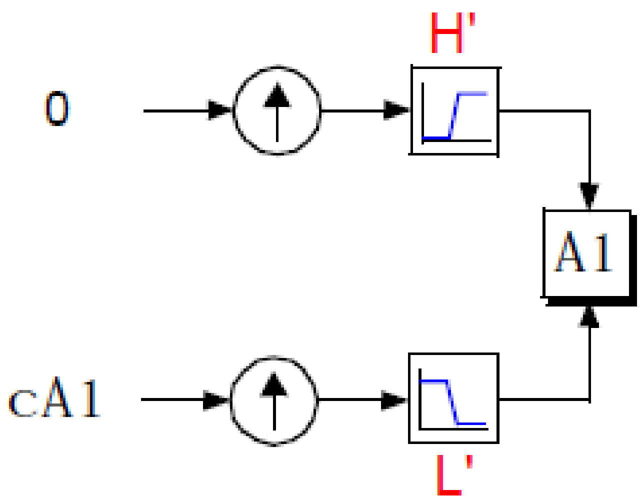

Fig. 2 Scheme of creating first level approximate signal from its coefficients

Table 1 Maximum responses of time history analysis applying coefficient and approximate records

No. of DOF	Dynamic analysis using cA2 record with 672 points			Dynamic analysis using A2 record with 672 points			Dynamic analysis using cA3 record with 338 points			Dynamic analysis using A3 record with 338 points		
	X direction Disp.	Y direction Disp.	Rotation	X direction Disp.	Y direction Disp.	Rotation	X direction Disp.	Y direction Disp.	Rotation	X direction Disp.	Y direction Disp.	Rotation
1	12.7592	3.3524	0.0056	12.7813	3.3592	0.0057	11.0168	2.8369	0.0046	11.1648	2.8741	0.0046
7	10.7972	1.0579	0.0059	10.8154	1.066	0.0059	9.3008	0.8238	0.0047	9.4279	0.8246	0.0047
10	8.6942	0.9854	0.0062	8.7083	0.9873	0.0063	7.5041	0.8259	0.0049	7.6081	0.8371	0.0044
16	6.5504	2.9624	0.0069	6.5606	2.9846	0.0069	5.7042	2.2744	0.0052	5.7836	2.2766	0.0052
18	4.4585	0.7259	0.0058	4.465	0.7272	0.0059	3.9558	0.6088	0.0043	4.0101	0.6172	0.0043
24	2.5437	1.905	0.0056	2.5471	1.9191	0.0056	2.3372	1.4344	0.004	2.3679	1.4361	0.004
26	0.9468	0.2711	0.003	0.948	0.2716	0.003	0.9257	0.2271	0.0022	0.9366	0.2303	0.0023
Time(s)	0.704499			0.704499			0.544896			0.544896		

Table 2 Minimum responses of time history analysis applying coefficient and approximate records

No. of DOF	Dynamic analysis using cA2 record with 672 points			Dynamic analysis using A2 record with 672 points			Dynamic analysis using cA3 record with 338 points			Dynamic analysis using A3 record with 338 points		
	X direction Disp.	Y direction Disp.	Rotation	X direction Disp.	Y direction Disp.	Rotation	X direction Disp.	Y direction Disp.	Rotation	X direction Disp.	Y direction Disp.	Rotation
1	-12.4863	-3.2952	-0.0061	-12.5824	-3.3207	-0.0061	-9.5841	-2.5962	-0.0053	-9.5966	-2.5987	-0.0054
7	-10.7427	-1.0479	-0.0062	-10.8243	-1.0501	-0.0062	-8.1383	-0.8785	-0.0053	-8.1493	-0.8903	-0.0054
10	-8.7422	-1.0004	-0.0063	-8.8081	-1.0079	-0.0063	-6.5434	-0.7756	-0.0053	-6.5528	-0.7763	-0.0054
16	-6.5667	-2.9003	-0.0066	-6.6161	-2.9059	-0.0066	-4.8686	-2.4367	-0.0055	-4.8765	-2.47	-0.0056
18	-4.3419	-0.747	-0.0055	-4.3752	-0.7525	-0.0055	-3.2123	-0.5719	-0.0047	-3.2183	-0.5725	-0.0047
24	-2.289	-1.8484	-0.0053	-2.3075	-1.8517	-0.0053	-1.76	-1.5656	-0.0046	-1.803	-1.5874	-0.0046
26	-0.7441	-0.283	-0.0033	-0.7466	-0.2851	-0.0033	-0.7016	-0.2143	-0.003	-0.6895	-0.2145	-0.003
Time(s)	0.704499			0.704499			0.544896			0.544896		

instead of using coefficient records, approximate records are utilized for dynamic analysis with these advantages:

I) The prescribed time intervals of time history analysis can be utilized for every *mother wavelet* and there are no *downsampling* effects on the time intervals.

II) Frequency content of every approximate record can be evaluated and compared easily due to identical record length without any shifting and scaling.

III) After dynamic analysis, response is determined and there is no need to implement inverse wavelet transform.

Results of the analysis for the seven-story steel moment frame under El Centro earthquake record shown in Fig. 5 are provided in Table 1 and Table 2 demonstrating the efficiency and accuracy of the presented approach. In the following sections, this approach is employed for approximate time history analysis.

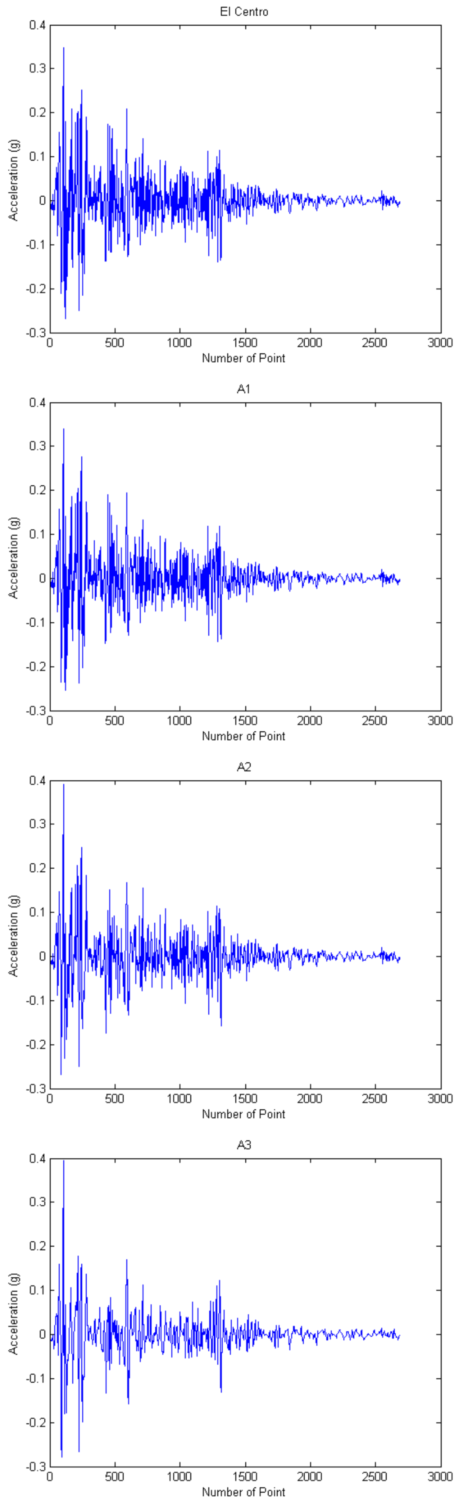

Fig. 3 El Centro earthquake record and its decompositions (Approximate records A1,A2, A3)

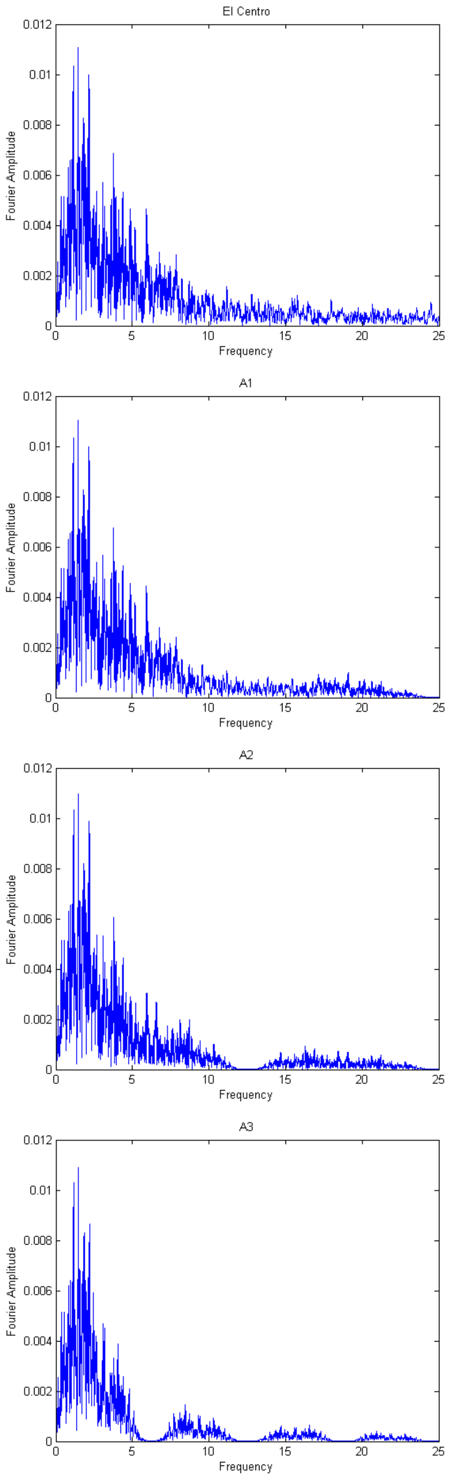

Fig. 4 Frequency content of El Centro earthquake record and its decompositions (Approximate records A1, A2, A3)

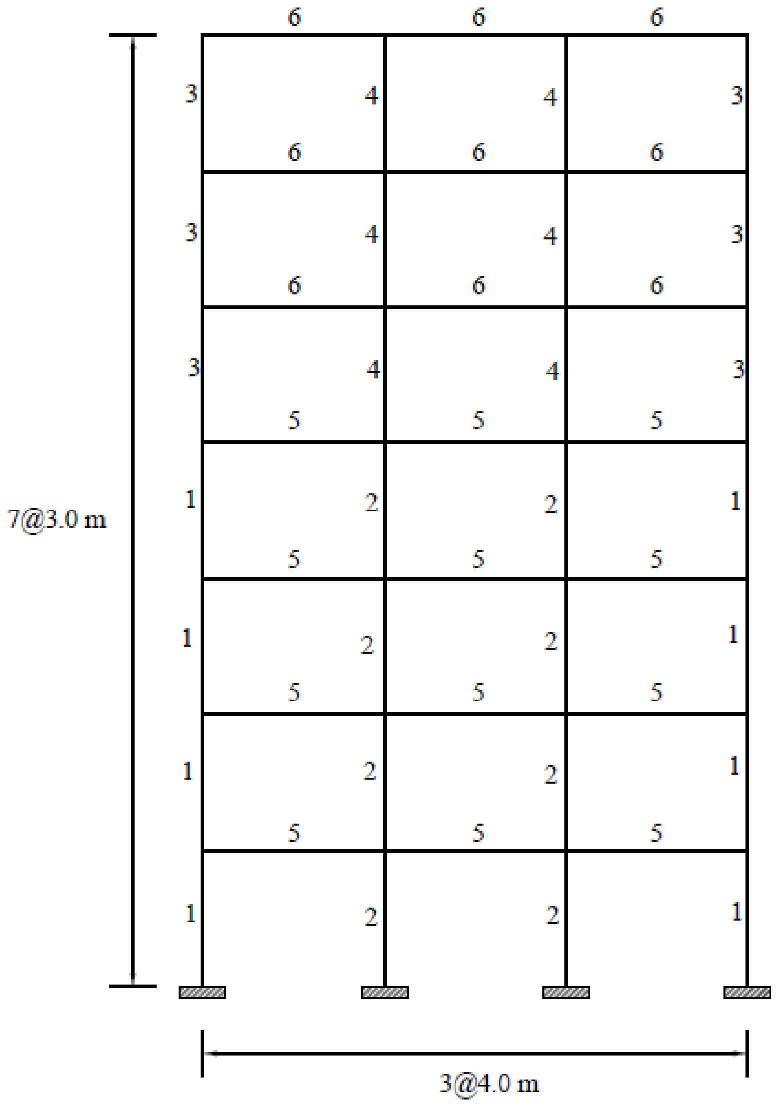

Fig. 5 Schematic of a seven-story steel moment frame

3.2 Reduced earthquake record for dynamic analysis

Here, approximate records (A1, A2, and A3) are utilized for dynamic analyses obtained from El Centro record. Hence, time intervals of dynamic analyses are chosen as 0.04, 0.08, and 0.16 seconds, respectively. Obviously, time intervals of original record are equal to 0.02. Newmark-Beta method (average acceleration) is employed for linear elastic time history analyses.

For linear elastic time history analysis, the analyst usually wants to find the maximum/minimum responses of the structures. Therefore, the time history analysis can be performed until the time point when the maximum/minimum response is obtained.

Four types of the seven-story frame with different fundamental natural frequencies and following relationship are considered: $\omega_1<\omega_2<\omega_3<\omega_4$

These frequencies are obtained by changing the stiffness of the frame. Results of the time history analysis of the frame types subjected to original record, A1, A2 and A3 are provided in Tables 3-6 possessing time point numbers corresponding to maximum and minimum responses for every lateral transitional degrees of freedom. It is shown that for approximate records, time points number values are identical or greater than time points number values of original record, particularly for A3. This means that if A3 is used for the dynamic analysis, an upper bound is created. In another words, extermum response subjected to original record occurs in an earlier time points. This is because of the filtering of the record by wavelet high pass filter. Some exceptions

Table 3 Point numbers corresponding to maximum (left) and minimum (right) response for first frame (ω_1)

Original	A1	A2	A3	Original	A1	A2	A3
272	272	274	274	306	306	306	306
272	272	274	274	306	306	306	306
272	272	274	274	306	306	306	306
272	272	274	274	306	306	306	306
273	274	274	274	306	306	306	306
273	274	274	274	306	306	306	306
273	274	274	274	306	306	306	306
273	274	274	274	306	306	306	306
274	274	274	274	307	308	306	306
274	274	274	274	307	308	306	306
274	274	274	274	307	308	306	306
274	274	274	274	307	308	306	306
274	274	274	274	307	308	306	306
274	274	274	274	307	308	306	306
274	274	274	274	307	308	306	306
274	274	274	274	307	308	306	306
273	274	274	274	307	306	306	306
273	274	274	274	307	306	306	306
273	274	274	274	307	306	306	306
273	274	274	274	307	306	306	306
272	272	270	274	305	306	306	314
272	272	270	274	305	306	306	314
272	272	270	274	305	306	306	314
272	272	270	274	305	306	306	314
270	270	270	***258***	303	304	306	314
270	270	270	***258***	303	304	306	314
270	270	270	***258***	303	304	306	314
270	270	270	***258***	303	304	306	314

Table 4 Point numbers corresponding to maximum (left) and minimum (right) response for second frame (ω_2)

Original	A1	A2	A3	Original	A1	A2	A3
142	142	142	146	118	118	170	170
142	142	142	146	118	118	170	170
142	142	142	146	118	118	170	170
142	142	142	146	118	118	170	170
142	142	142	146	117	118	118	170
142	142	142	146	117	118	118	170
142	142	142	146	117	118	118	170
142	142	142	146	117	118	118	170
142	142	142	146	116	116	118	218
142	142	142	146	116	116	118	218
142	142	142	146	116	116	118	218
142	142	142	146	116	116	118	218
142	142	142	146	116	116	118	218
142	142	142	146	116	116	118	218
142	142	142	146	116	116	118	218
142	142	142	146	116	116	118	218
142	142	142	146	169	170	170	218
142	142	142	146	169	170	170	218
142	142	142	146	169	170	170	218
142	142	142	146	169	170	170	218
142	144	142	146	169	218	218	218
142	144	142	146	169	218	218	218
142	144	142	146	169	218	218	218
142	144	142	146	169	218	218	218
144	144	142	146	218	218	218	218
144	144	142	146	218	218	218	218
144	144	142	146	218	218	218	218
144	144	142	146	218	218	218	218

are highlighted in Table 3 but it does not change the result, because maximum points number values from all lateral degrees of freedom (corresponding to maximum/minimum response) is selected as a *critical point number. Critical point number* is a time point that time history analysis is terminated until that point, while extermum response has been obtained.

In another aspect, Figs. 6-9 show the point number where the maximum or minimum response occurs. Each line illustrates maximum or minimum response of one type of frame with a certain fundamental frequency. Clearly, greater point numbers are visible for the frame with lesser fundamental frequency.

By employing El Centro, A1, A2 and A3 records, these figures demonstrate that with dynamic

Table 5 Point numbers corresponding to maximum (left) and minimum (right) response for third frame (ω_3)

Original	A1	A2	A3	Original	A1	A2	A3
134	134	134	138	113	114	114	290
134	134	134	138	113	114	114	290
134	134	134	138	113	114	114	290
134	134	134	138	113	114	114	290
134	134	134	138	113	114	114	290
134	134	134	138	113	114	114	290
134	134	134	138	113	114	114	290
134	134	134	138	113	114	114	290
98	134	134	138	113	114	114	290
98	134	134	138	113	114	114	290
98	134	134	138	113	114	114	290
98	134	134	138	113	114	114	290
98	134	134	138	113	114	114	290
98	134	134	138	113	114	114	290
98	134	134	138	113	114	114	290
98	134	134	138	113	114	114	290
134	134	134	138	113	114	114	290
134	134	134	138	113	114	114	290
134	134	134	138	113	114	114	290
134	134	134	138	113	114	114	290
133	134	134	138	112	112	114	290
133	134	134	138	112	112	114	290
133	134	134	138	112	112	114	290
133	134	134	138	112	112	114	290
133	134	134	138	110	110	114	290
133	134	134	138	110	110	114	290
133	134	134	138	110	110	114	290
133	134	134	138	110	110	114	290

analysis of frame via smaller natural fundamental frequency, greatest time point number is achieved, and after that one can utilize this type in order to gain maximum response of different types of the frame structure.

During the size optimization procedure, cross-section areas of members are changed, so a time point corresponding to extermum response values should be considered in such a way that during this procedure a reliable time point for the entire generated frames (determined from variables' domain) is achieved. Thus, if A3 record has been employed for analyses, an upper bound of *critical point number* has been created. Also, considering a generated frame with minimum frequency before the beginning of a size structural optimization, the imposed constraints' values due to the time history dynamic analysis are acceptable i.e., the extermum responses of the entire

Table 6 Point numbers corresponding to maximum (left) and minimum (right) response for forth frame (ω_4)

Original	A1	A2	A3	Original	A1	A2	A3
94	94	258	130	109	110	110	114
94	94	258	130	109	110	110	114
94	94	258	130	109	110	110	114
94	94	258	130	109	110	110	114
94	94	258	130	109	110	110	114
94	94	258	130	109	110	110	114
94	94	258	130	109	110	110	114
94	94	258	130	109	110	110	114
94	94	258	130	110	110	110	114
94	94	258	130	110	110	110	114
94	94	258	130	110	110	110	114
94	94	258	130	110	110	110	114
94	94	258	130	110	110	110	114
94	94	258	130	110	110	110	114
94	94	258	130	110	110	110	114
94	94	258	130	110	110	110	114
94	94	94	130	109	110	110	114
94	94	94	130	109	110	110	114
94	94	94	130	109	110	110	114
94	94	94	130	109	110	110	114
94	94	94	130	109	110	110	114
94	94	94	130	109	110	110	114
94	94	94	130	109	110	110	114
94	94	94	130	109	110	110	114
93	94	258	130	109	108	110	114
93	94	258	130	109	108	110	114
93	94	258	130	109	108	110	114
93	94	258	130	109	108	110	114

generated frames occur in an identical or earlier point number relative to the *critical point number*. Some exceptions of frames ω_1, ω_2 are visible in Figs. 8 and 9. These exceptions are negligible by imposing two frequency constraints consisting of lower bound and upper bound frequency constraints.

Fundamental steps of applying reduced record to the dynamic design optimization can be summarized as follows:

1) From available cross-section areas, assign smallest cross-section to all members of the frame (weakest available frame). Perform a time history analysis subjected to A3 record and determine the point number corresponding to extremum absolute value of response (maximum or minimum) denoted P_l. Also, store the fundamental natural frequency of the structure denoted by ω_l.

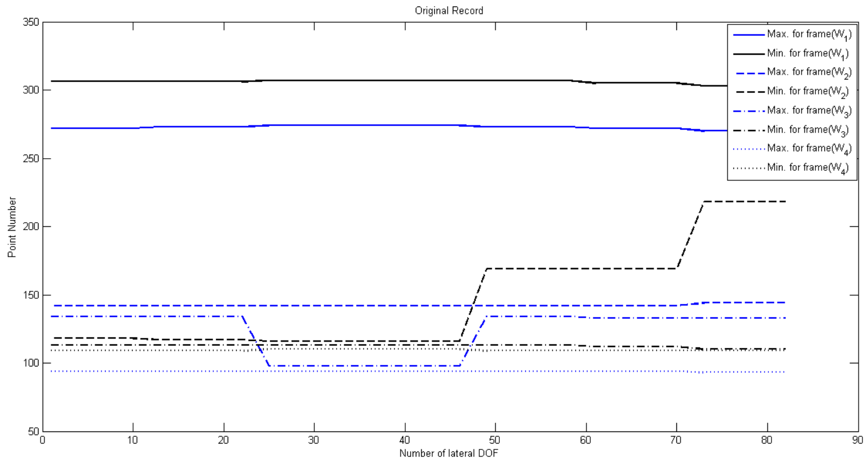

Fig. 6 Time points corresponding to max/min responses versus lateral DOFs under original record

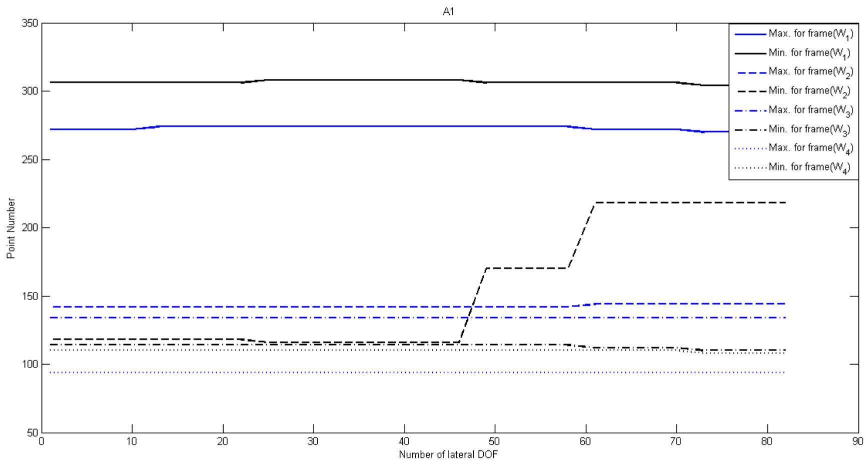

Fig. 7 Time points corresponding to max/min responses versus lateral DOFs under approximate record (A1)

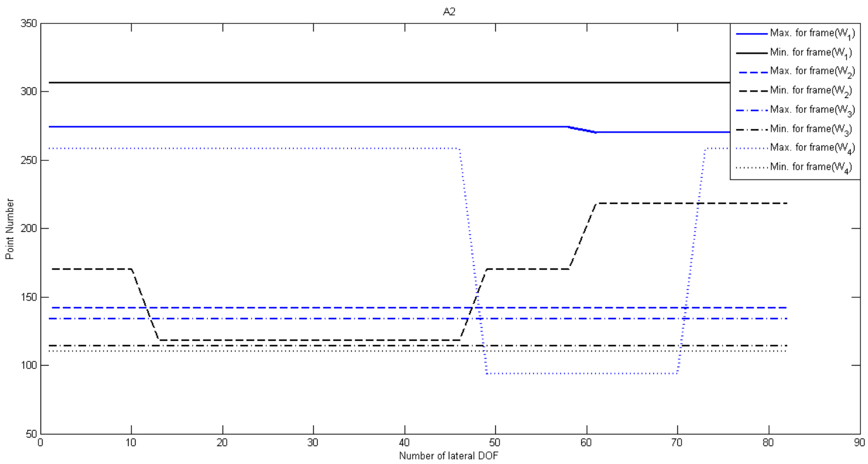

Fig. 8 Time points corresponding to max/min responses versus lateral DOFs under approximate record (A2)

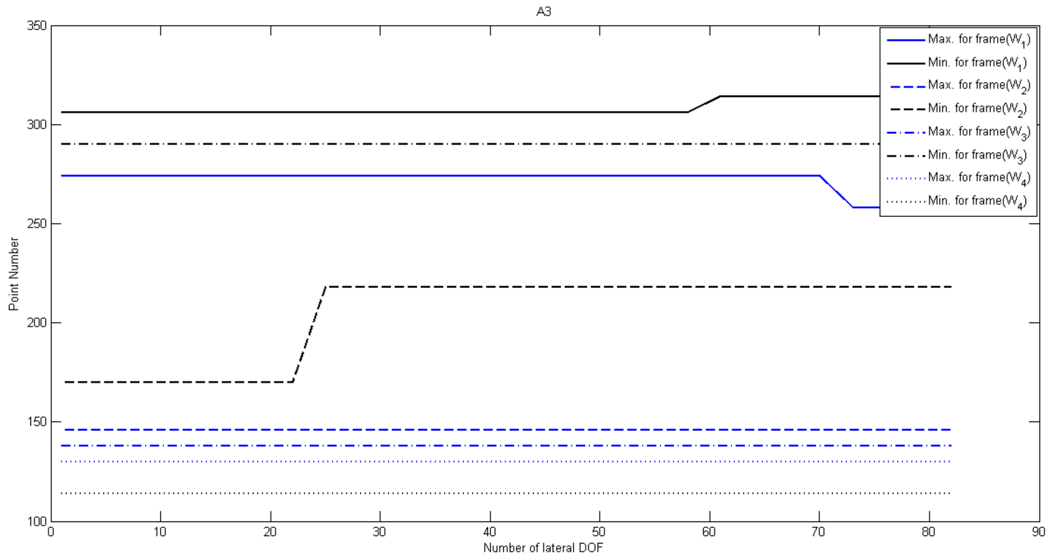

Fig. 9 Time points corresponding to max/min responses versus lateral DOFs under approximate record (A3)

2) From available cross-section areas, assign the largest cross-section to all members of the frame (strongest available frame). Perform a time history analysis subjected to A3 record and determine the point number corresponding to extremum absolute value of response (maximum or minimum) denoted P_u. Store the fundamental natural frequency of the structure denoted by ω_u as well.

3) Determine the critical point number which is equal to $P_{critical}$=max(P_l, P_u).

4) Here, a reduced record is the original record that is utilized for time history analysis until a time step or the time point equal to $P_{critical}$ considering the original time intervals (e.g., 0.02 for El Centro record).

5) In order to have a reliable critical time point during the optimization procedures, impose two frequency constraints from predetermined values of the first and second steps as follows

$$\begin{aligned} &upperbound \qquad && \omega < \omega_u \\ &lowerbound \qquad && \omega > \omega_l \end{aligned} \tag{7}$$

ω denotes the fundamental frequency of the structure in the current iteration of optimization. These frequency constraints make sure us that during the optimization iterations, there is no maximum response of the generated frame structure occurring after the determined critical point.

Reduced Record Method (RRM) has four major advantages including:

a) Instead of an approximate record, the original record is applied for dynamic analysis in the optimization procedures. Therefore, dynamic responses are exact (non-approximate).

b) Obviously, time intervals are clearly defined.

c) Computational effort is greatly decreased to about 25 percent of usual analysis.

d) There is no more need to implement inverse wavelet transforms throughout the process of optimization.

Optimal design of a frame incorporating the proposed methodology is mentioned in sixth section as an example. An improved version of harmony search meta-heuristic algorithm is used as an optimizer, (Mahdavi *et al*. 2007). This method is briefly discussed in following section.

4. An improved harmony search

4.1 Harmony search

Geem *et al*. (2001), Lee and Geem (2004, 2005) presented Harmony Search (HS) algorithm which is briefly explained here, more information can be found in the mentioned references. This meta-heuristic algorithm was inspired by the process of composing music. A composer wants to reach a perfect harmony status in music improvisation. Seeking for pleasant harmonies in composing is similar to finding an optimum solution in optimization problems. Generation of a new harmony is called improvisation. An improvement on this algorithm is carried out by Mahdavi *et al*. (2007) leading to the Improved Harmony Search (IHS). Here, a discrete edition of the IHS is used (Kaveh and Zakian 2013), consisting of the following steps:

Step 1: Initialization

Initial random values in their domain are determined. The parameters of the algorithm consist of the *HMS* (Harmony Memory Size), number of variables *nv*, Harmony Memory Considering Rate (*HMCR*), Pitch Adjusting Rate (*PAR*), and the maximum number of iterations or terminating criterion. HMCR is a fixed value in the range of 0.70-0.95. In this paper, HMCR is taken as 0.95.

Step 2: Initialize the harmony memory

In this step the harmony memory is filled with some random solution vectors.

Step 3: Improvise a new harmony

A new harmony vector is specified by the following three criteria:

(1) Using harmony memory,

(2) Pitch adjustment,

(3) Random selection.

In using the harmony memory, the value of the first decision variable for the new vector is chosen from any of the values in the specified *HM* range. The *HMCR* is the rate of considering one value from the historical values stored in the *HM*, while (1–*HMCR*) is the rate of randomly selected value from the possible range of values. $x_{\min,j}$, $x_{\max,j}$ are lower and upper limits of the variable *j*, respectively.

$$x_{i,j} \Leftarrow \begin{cases} x_{i,j} \in HM & with\ probability\ \ HMCR \\ x_{i,j} \in [x_{\min,j}, x_{\max,j}] & with\ probability\ \ (1-HMCR) \end{cases} \tag{8}$$

Then every component achieved by the memory consideration must be tested to determine whether it should be pitch-adjusted. This operation utilizes the *PAR* parameter, which is the rate of pitch adjustment as follows

$$pitch\ adjusting\ decision\ \ for\ x_{i,j} \Leftarrow \begin{cases} yes & with\ probability\ \ PAR \\ no & with\ probability\ \ (1-PAR) \end{cases} \tag{9}$$

The value of (1-*PAR*) sets the rate of doing nothing. If the pitch adjustment decision for $x_{i,j}$ is *yes*, then $x_{i,j}$ is replaced as follow

$$x_{i,j} = RoundD(x_{i,j} \pm rand * bw) \tag{10}$$

Here, *bw* is the bandwidth that controls the local domain of the pitch adjustment. *RoundD* rounds the solution to the nearest admissible available discrete value.

Step 4: Update harmony memory

If the new harmony vector is better than the worst harmony in the *HM*, based on the objective function, the new generated harmony is included in the *HM* and the existing worst one is excluded from *HM*.

Step 5: Terminating criterion

If the fulfilling criterion (maximum number of iterations) is satisfied, computation is terminated. Otherwise, Steps 3 and 4 are repeated again.

4.2 *Improved harmony search*

The difference between the classic version and improved version is that in the classic method two parameters of *PAR* and *bw* are constant. However, in the improved version which was presented by Mahdavi *et al*. (2007), the *PAR* and *bw* are linear increasing and nonlinear decreasing relationships with the increment of the iteration, respectively. The basic advantage of the aforementioned improvement is that by careful adjustment of these parameters, one can reduce the number of iterations as well. Small *PAR* and big *bw* values lead to diversity of the algorithm and exploration ability of the algorithm is provided. Big *PAR* and small *bw* values lead to improvement of the solutions in the last iterations resulting is a much better convergence. Here, for a favorable performance PAR_{min} and PAR_{max} are selected as 0.35 and 0.99, respectively. These parameters are updated as follows

$$PAR(iter) = PAR_{\min} + \frac{(PAR_{\max} - PAR_{\min})}{iter_{\max}} \cdot iter \tag{11}$$

$$bw(iter) = bw_{\max} \exp\left(\frac{Ln\left(\frac{bw_{\min}}{bw_{\max}}\right)}{iter_{\max}} \cdot iter\right) \tag{12}$$

where, *Iter* is the iteration number, $Iter_{max}$ is the maximum number of iterations, *PAR(iter)* is the pitch adjusting rate at current iteration, PAR_{min} is the minimum pitch adjusting rate, PAR_{max} is the maximum pitch adjusting rate, *bw*(*iter*) is the bandwidth for current iteration, bw_{min} is the minimum bandwidth, and bw_{max} is the maximum bandwidth.

5. Formulation of dynamic drift design optimization

Structural design optimization problems can be divided into three categories: size optimization, shape (geometry) optimization, topology optimization. In the size optimization that is the concern of this paper usually design variables are in the form of thickness or dimensions of the members of the structure.

For practical reasons, the cross-section areas of the structural members are considered as design variables, which are selected from a list of available sections. The discrete optimization is formulated as follows

$$\begin{aligned}&\mathit{Minimize}\quad \mathrm{f(X)}\\&\text{subject to}\ \ \mathrm{g_j(X)} \le 0\\&\mathrm{X} = [\mathrm{x_1, x_2, ..., x_{nv}}]\\&\mathrm{i} = 1,2,...\mathrm{nv}\\&\mathrm{x_i} \in \mathrm{R^d}\end{aligned} \tag{13}$$

$$to\,minimize\ \ Obj(X) = f(X) \times f_{penalty}(X) \tag{14}$$

where X is the vector of design variables containing the cross section areas, nv is the number of design variables or the number of member groups, and R^d is the domain of the design variables.

Here, $Obj(X)$ is the objective function, $f(X)$ is the structural weight function, and $f_{\mathrm{penalty}}(X)$ is penalty function in order to control the constraints

$$f(X) = \sum_{i=1}^{nv} \gamma_i \cdot x_i \cdot l_i \tag{15}$$

$$f_{penalty}(X) = (1 + \kappa_1 \cdot \nu)^{\kappa_2}\ ,\ \ \nu = \sum_{i=1}^{n} \max[0, \nu_i] \tag{16}$$

l_i is the member length, and γ_i is the material density of the member i. Here, the parameters κ_1 and κ_2 for the penalty function are selected as 1 and 2, respectively. ν represents the sum of the violated constraints.

Design constraints are as follows:

Drift constraints

$$\frac{\delta_i - \delta_{i-1}}{h_i} < DR_a \quad i = 1,2,...,ns \tag{17}$$

where δ_i is the lateral displacement of the center of the mass in the story i, h_i is the height of the story i, and DR_a is the allowable drift ratio of each story. ns is the number of the frame stories. This constraint is time-dependent, and it is handled by a conventional method as described in Kocer and Arora(1999). In this method, the time interval is divided into subintervals and the time-dependent constraints are imposed at grid points.

Dynamic equilibrium equation of a moment resisting frame subjected to seismic loading can be expressed as

$$M\,\ddot{u}(t) + C\,\dot{u}(t) + K\,u(t) = -p\,\ddot{u}_g(t)$$

$$p = \begin{cases} p_k = m_{kx} & \scriptstyle for\ x\,direction\,DOFs \\ p_k = 0 & \scriptstyle else \end{cases} \qquad \textit{for moment frame} \tag{18}$$

where M, C and K are the mass, damping, and stiffness matrix of the structure, respectively. $\ddot{u}(t)$, $\dot{u}(t)$, $u(t)$ are the acceleration, velocity and displacement vectors. p_k is the kth array of the p

matrix, m_{kx} denotes the assigned lumped mass of the kth DOF at x direction. $\ddot{u}_g(t)$ is the ground acceleration scalar value at the time t, and p is a column matrix. Newmark-Beta integration method is used for dynamic analysis, and for damping matrix, the Rayleigh relationship is employed in the analysis. More information on this relationship can be found in Clough and Penzien (2003). Dynamic analysis, and optimization algorithms are all programmed in *Matlab* and Wavelet analysis are accomplished with *Matlab Wavelet Toolbox*, Misiti *et al*. (2005).

6. Structural design optimization examples

In this part, optimal design of a frame structure is accomplished using available cross-section database Table 7.

Based on cross-section database**,** eigenvalue analysis of the two structures with weakest members corresponding to minimum fundamental frequency of the structure and with strongest members corresponding to maximum fundamental frequency of the structure is performed.

ω_l=4.0292 Hz is the achieved fundamental natural frequency of a frame corresponding to weakest (minimum stiffness) frame considering aforementioned database.

ω_u=14.0019 Hz is the achieved fundamental natural frequency of a frame corresponding to strongest frame (maximum stiffness) considering aforementioned database.

6.1 Optimal design under El Centro record

For determining the critical time point weakest and strongest frame are analyzed under the A3 record of El Centro:

P_l =274 is the point number corresponding to maximum response time point.

P_u=314 is the point number corresponding to minimum response time point.

Say $P_{critical}$ =320th point as a critical one which is implemented in the optimization procedure.

Thus, all analyses are accomplished using only 320 steps of the dynamic analysis incorporating original record considering two frequency constraints.

Table 7 Cross-section database

No	Profile	Area (cm^2)	Moment of Inertia (cm^4)	No	Profile	Area (cm^2)	Moment of Inertia (cm^4)
1	IPE240	39.1	3890	11	IPB300	149	25170
2	IPE270	45.9	5790	12	IPB320	161	30820
3	IPE300	53.8	8360	13	IPB340	171	33660
4	IPE330	62.6	11770	14	IPB360	181	43190
5	IPE360	72.7	16270	15	IPB400	198	57680
6	IPB200	78.1	5700	16	IPB450	218	79890
7	IPB220	91	8090	17	IPB500	239	107200
8	IPB240	106	11260	18	IPB550	254	136700
9	IPB260	118	14920	19	IPB600	270	171000
10	IPB280	131	19270	20	IPB650	286	210600

The seven-story moment frame is considered as an example and design variables consisting of four columns and two beams groups are defined in Fig. 5. El Centro record is employed for time history analysis. Modulus of elasticity, weight density and damping ratio are equal to 2.06×10^{7} N/cm^{2}, 0.077 $N/cm^{3}$and 0.2, respectively. Total mass matrix of the structure consists of global structural members' mass matrix plus lumped mass matrix. 2000 kg lumped masses only have been assigned to all transitional degrees of freedom. The only constraint is drift ratio that is imposed to all stories of the frame and is limited to 0.005. It should be noted that when reduced record method is used, two frequency constraints should be added. Results of optimization applying original record and reduced record are provided in Table 8 demonstrating significant computational effort reduction. Clearly, there is no inappropriate change in the optimization path after using RRM based on Fig. 10 and Table 8. Moreover, Fig. 11, Fig. 12 and Table 9 show that for both applied records, no constraints are violated. It should be noticed that in Fig. 12 and Table 9, the original record has been employed for constraint violation checking. Fundamental frequency of the optimal frame structure obtained incorporating reduced record is equal to 12.2236 Hz meaning that the frequency constraints are not violated.

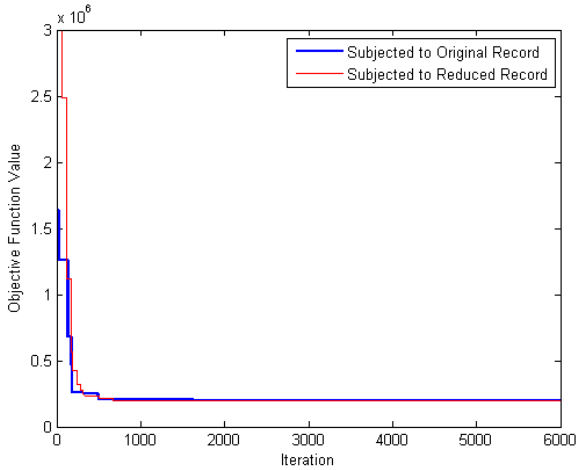

Fig. 10 Convergence history of optimization incorporating two different records of El Centro

Table 8 Optimum solution of IHS incorporating two different records of El Centro

Group No.	Optimum cross-section area employing the original record (cm^2)	Optimum cross-section area employing the reduced record (cm^2)
1	181	181
2	270	254
3	181	181
4	270	254
5	270	286
6	198	198
Weight(N)	**197410**	**194210**
Optimization Time (min)	**129**	**20**

Table 9 Drift ratios of the optimum frame structure under El Centro seismic loading

Story No.	Drift ratios of optimum frame structure employing the original record	Drift ratios of optimum frame structure employing the reduced record
1	0.0039	0.0042
2	0.0050	0.0049
3	0.0049	0.0047
4	0.0045	0.0043
5	0.0047	0.0047
6	0.0047	0.0047
7	0.0034	0.0034

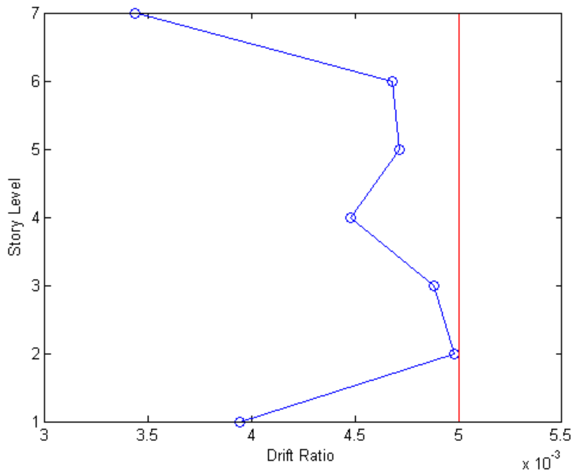

Fig. 11 Maximum drift ratios of optimum solution achieved by dynamic analysis using original record of El Centro

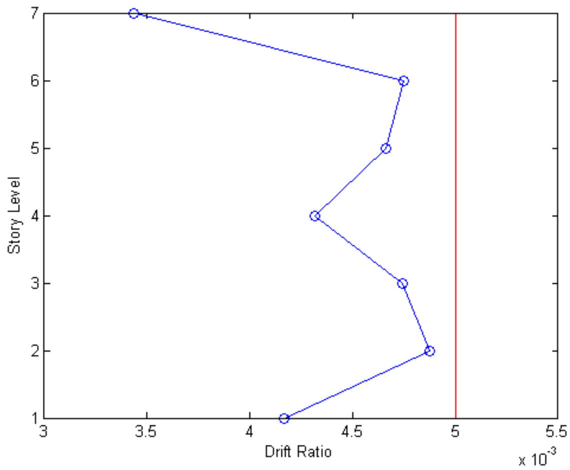

Fig. 12 Maximum drift ratios of optimum solution achieved by dynamic analysis using reduced record of El Centro

6.2 Optimal design under Kobe record

Here, Kobe earthquake record (Fig. 13) with 4096 time points and time intervals of 0.01 are applied to the frame structure so as to perform better assessment of proposed methodology. All of the properties of the frame are such as previous part. Here, Drift constraint is restricted to 0.005 as well.

For determining the critical time point, the weakest and strongest frame are analyzed under the A3 record of Kobe:

P_l=866 is the point number corresponding to maximum response time point.

P_u=938 is the point number corresponding to minimum response time point.

Say $P_{critical}$=940th point as a critical one that is imposed in the optimization procedure. Therefore, all analyses are accomplished using just 940 steps of the dynamic analysis incorporating original record considering two frequency constraints.

Outcomes of optimization applying original record and reduced record are provided in Table 10 demonstrating significant computational effort reduction. Not only there is no inappropriate change in the optimization path after using RRM based on Fig. 14 and Table 10, but also Fig. 15 and Table 11 illustrate that for both applied records, no constraints are violated. Fundamental frequency of the optimal frame structure obtained incorporating reduced record is equal to 6.9461 Hz which means that the frequency constraints are not violated.

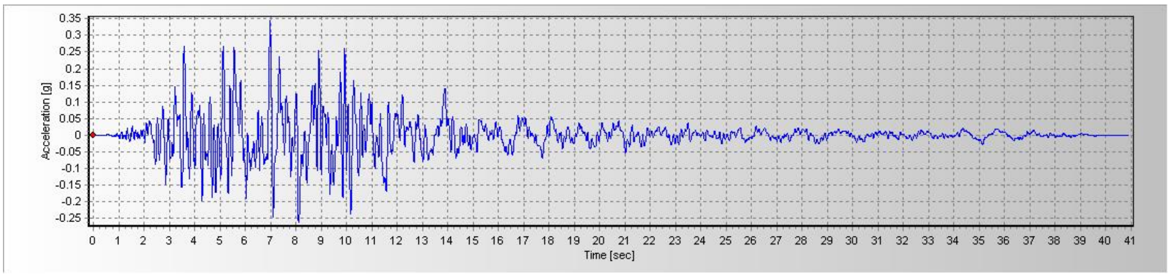

Fig. 13 Kobe earthquake record

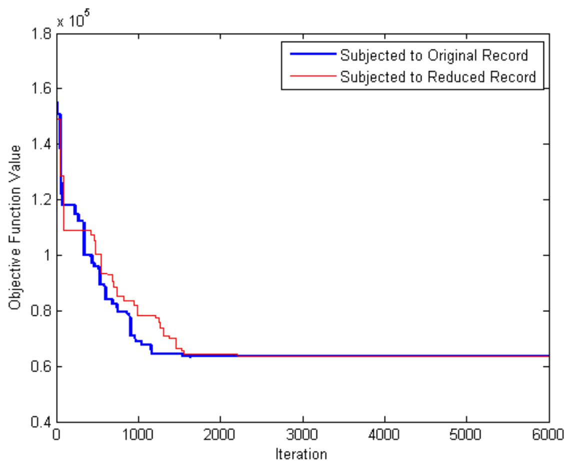

Fig. 14 Convergence history of optimization incorporating two different records of Kobe

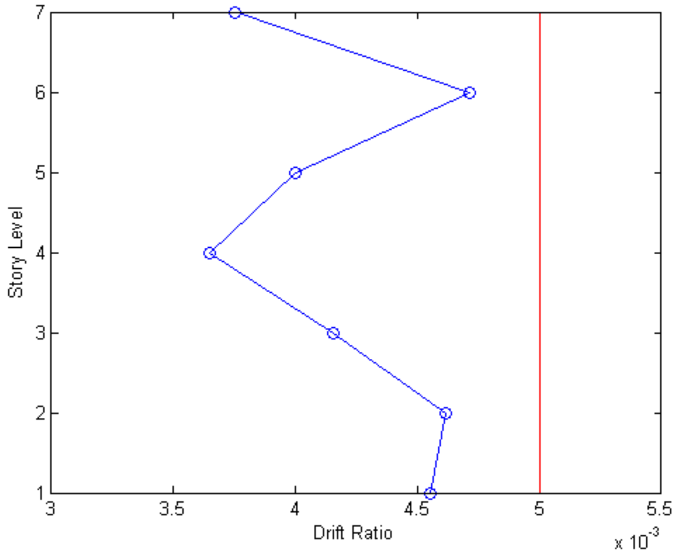

Fig. 15 Maximum drift ratios of optimum solution achieved by dynamic analysis using original record and reduced record of Kobe

Table 10 Optimum solution of IHS incorporating two different records of Kobe

Group No.	Optimum cross-section area employing the original record (cm^2)	Optimum cross-section area employing the reduced record (cm^2)
1	53.8	53.8
2	72.7	72.7
3	53.8	53.8
4	72.7	72.7
5	149	149
6	45.9	45.9
Weight(N)	**635080**	**635080**
Optimization Time (min)	**201**	**52**

Table 11 Drift ratios of the optimum frame structure under Kobe seismic loading

Story No.	Drift ratios of optimum frame structure employing the original record	Drift ratios of optimum frame structure employing the reduced record
1	0.0046	0.0046
2	0.0046	0.0046
3	0.0042	0.0042
4	0.0037	0.0037
5	0.0040	0.0040
6	0.0047	0.0047
7	0.0038	0.0038

7. Conclusions

In this article, a new approach is proposed for approximate time history analysis of skeletal structures, and then by using this method a methodology so-called *reduced record method (RRM)* is proposed based on approximate prediction of time points corresponding to extermum response of the original record. RRM can be used for linear elastic time history analysis of structures during the optimization procedures when maximum/minimum responses are under consideration. RRM inputs no approximation to the dynamic analysis of the structures, and only determination of the critical point number is the vital phase of this method. This method employs a selected original record and performs time history analysis until the obtained critical time point of this selected record. The presented method reduces the computational effort of time consuming optimization procedures associated with seismic analyses to about 25 percent of the time used in ordinary procedures.

Design example has demonstrated efficiency of proposed method. This method can be extended to the large-scale frame structures. More investigation should be accomplished for assessment of the RRM for other categories of skeletal structures such as trusses, grids and 3D frame structures.

Acknowledgements

The first author is grateful to the Iran National Science Foundation for the support.

References

Cheng, F.Y., Ger, J. and Li D. (2000), “Multiobjective optimization of seismic structures”, Ed. P.E. Mohamed Elgaaly, ASCE Structures Congress 2000, Amer. Soc. Civil Enger., Philadelphia, Pennsylvania, US.

Clough, R.W. and Penzien, J. (2003), “Dynamics of structures”, *Computers and Structures*, USA.

Gurley, K. and Kareem, A. (1999), “Applications of wavelet transforms in earthquake, wind and ocean engineering”, *Eng. Struct*., **21**, 149-167.

Kaveh, A., Fahimi-Farzam, M. and Kalateh-Ahani, M. (2012), “Time-history analysis based optimal design of space trusses: The CMA evolution strategy approach using GRNN and WA”, *Struct. Eng. Mech*., **44**, 379-403.

Kaveh, A. and Zakian, P. (2012), “Performance based optimal seismic design of RC shear walls incorporating soil-structure interaction using CSS algorithm”, *Int. J. Optim. Civil Eng*., **2**, 383-405.

Kaveh, A. and Zakian, P. (2013), “Optimal design of steel frames under seismic loading using two meta-heuristic algorithms”, *J. Construct. Steel Res*., **82**, 111-130.

Kaveh, A. and Zakian, P. (2014), “Enhanced bat algorithm for optimal design of skeletal structures”, *Asian J. Civil. Eng*., **15**, 179-212.

Kaveh, A. and Zolghadr, A. (2014), “Democratic PSO for truss layout and size optimization with frequency constraints”, *Comput. Struct*., **130**, 10-21.

Kocer, F. and Arora, J. (1999), “Optimal design of H-frame transmission poles for earthquake loading”, *J. Struct. Eng*., **125**, 1299-1308.

Gholizadeh, S. and Barzegar, A. (2013), “Shape optimization of structures for frequency constraints by sequential harmony search algorithm”, *Eng. Optim*., **45**, 627-646.

Gholizadeh, S. and Salajegheh, E. (2009), “Optimal design of structures subjected to time history loading by

swarm intelligence and an advanced metamodel", *Comput. Meth. Appl. Mechan. Eng*., **198**, 2936-2949.
Gholizadeh, S. and Samavati, O.A. (2011), "Structural optimization by wavelet transforms and neural networks", *Appl. Math. Model*., **35**, 915-929.
Lee, K.S. and Geem, Z.W. (2004), "A new structural optimization method based on the harmony search algorithm", *Comput. Struct*., **82**, 781-798.
Lee, K.S. and Geem, Z.W. (2005), "A new meta-heuristic algorithm for continuous engineering optimization: harmony search theory and practice", *Comput. Meth. Appl. Mech. Eng*., **194**, 3902-3933.
Mahdavi, M., Fesanghary, M. and Damangir, E. (2007), "An improved harmony search algorithm for solving optimization problems", *Appl. Math. Comput*., **188**, 1567-1579.
Misiti, M., Misiti, Y., Oppenheim, G. and Poggi, J. (2005), Matlab, Wavelet Toolbox User's guide version 3.
Prendes, Gero, M.B., Bello, García, A. and del Coz, Díaz, J.J. (2005), "A modified elitist genetic algorithm applied to the design optimization of complex steel structures", *J. Construct. Steel Res*., **61**, 265-280.
Prendes, Gero, M.B., García, A.B. and del, Coz, Díaz, J.J. (2006), "Design optimization of 3D steel structures: Genetic algorithms vs. classical techniques", *J. Construct. Steel Res*., **62**, 1303-1309.
Salajegheh, E., Heidari, A. and Saryazdi, S. (2005), "Optimum design of structures against earthquake by discrete wavelet transform", *Int. J. Numer. Meth. Eng*., **62**, 2178-2192.
Salajegheh, E. and Heidari, A., (2005a), "Time history dynamic analysis of structures using filter banks and wavelet transforms", *Comput. Struct*., **83**, 53-68.
Salajegheh, E. and Heidari, A. (2005b), "Optimum design of structures against earthquake by wavelet neural network and filter banks", *Earthq. Eng. Struct. Dyn*., **34**, 67-82.
Salajegheh, E. and Heidari, A. (2004), "Optimum design of structures against earthquake by adaptive genetic algorithm using wavelet networks", *Struct. Multidiscip. Optim*., **28**, 277-285.
Geem, Z.W., Kim, J.H. and Loganathan, G.V. (2001), "A new heuristic optimization algorithm: harmony search", *Simulation*, **76**, 60-68.
Zou, X.K. and Chan, C.M. (2005), "An optimal resizing technique for seismic drift design of concrete buildings subjected to response spectrum and time history loadings", *Comput. Struct*., **83**, 1689-1704.

CC